

DOI: 10.1002/chem.201202531

# Thicker is Better? Synthesis and Evaluation of Well-Defined Polymer Brushes with Controllable Catalytic Loadings

Antony E. Fernandes,<sup>[a]</sup> Ali Dirani,<sup>[a]</sup> Cécile d'Haese,<sup>[a]</sup> Gladys Deumer,<sup>[b]</sup>  
Weiming Guo,<sup>[a]</sup> Peter Hensenne,<sup>[a]</sup> Fady Nahra,<sup>[a]</sup> Xavier Laloyaux,<sup>[a]</sup>  
Vincent Haufroid,<sup>[b]</sup> Bernard Nysten,<sup>[a]</sup> Olivier Riant,<sup>\*[a]</sup> and Alain M. Jonas<sup>\*[a]</sup>

**Abstract:** Polymer brushes (PBs) have been used as supports for the immobilization of palladium complexes on silicon surfaces. The polymers were grown by surface-initiated atom-transfer radical polymerization (SI-ATRP) and postdecorated with dipyriddyamine (dpa) ligands. The pendant dpa units were in turn complexed with [Pd(OAc)<sub>2</sub>] to afford hybrid catalytic surfaces. A series of catalytic samples of various thicknesses (ca. 20–160 nm) and associated palladium loadings (ca. 10–45 nmol cm<sup>-2</sup>) were obtained by adjusting the SI-ATRP reaction time and characterized by ellipsometry, X-ray re-

flectivity, X-ray photoelectron spectroscopy, and inductively coupled plasma mass spectrometry (ICP-MS). ICP-MS revealed a near-linear relationship between thickness of the polymer brush and palladium content, which confirmed the robustness of the preparation and postmodification sequence presented herein, rendering possible the creation of functional architectures with predefined catalytic potential. The

**Keywords:** palladium • polymers • silicon • supported catalysts • surface chemistry

activities of the catalytic PBs were determined by systematically exploring a full range of substrate-to-catalyst ratios in a model palladium(0)-catalyzed reaction. Quantitative transformations were observed for loadings down to 0.03 mol % and a maximum turnover number (TON) of around 3500 was established for the system. Comparison of the catalytic performances evidenced a singular influence of the thickness on conversions and TONs. The limited recyclability of the hairy catalysts has been attributed to palladium leaching.

## Introduction

Polymer brushes (PBs)<sup>[1]</sup> represent versatile molecular constructions for shaping surface properties for applications in domains such as actuation,<sup>[2]</sup> electronics,<sup>[3]</sup> and biology.<sup>[4]</sup> Their interest lies in the possibility of finely adjusting the polymeric core composition of the brush together with the possibility of postfunctionalizing the pendant lateral chains towards their desired use. The covalent attachment of functional molecules (e.g., biomolecules,<sup>[5]</sup> switches,<sup>[6]</sup> and catalysts<sup>[7]</sup>) therefore provides access to a new class of hybrid devices. The dynamic nature of the PBs together with the par-

ticularly high local concentrations engendered with such frameworks offer unique opportunities in supported catalysis.<sup>[7]</sup> In some cases the PB architecture can significantly enhance the outcome of cooperative catalytic processes that require the close proximity of synergetic active sites.<sup>[7c]</sup> It is also possible to incorporate catalytic PB coatings inside the walls of microreactors for application in continuous flow processes.<sup>[7d,g,h]</sup>

In general, PBs are prepared by using the “grafting from” strategy, which encompasses the preliminary preparation of an initiator monolayer followed by surface-initiated “living” polymerization.<sup>[8]</sup> Modifying the polymerization conditions (e.g., solvent, concentration, reaction time) allows additional control over the thickness and architecture of the brushes, which can be particularly attractive for the configuration of well-defined structures with determined functional loadings.<sup>[7d,g,h]</sup> However, despite the remarkable potential of PBs, there are still very few applications in heterogeneous catalysis.<sup>[7]</sup>

Herein we report the robust, stepwise, construction and detailed examination of catalytic PBs prepared from single-crystal silicon surfaces and the impact of thickness on activity.

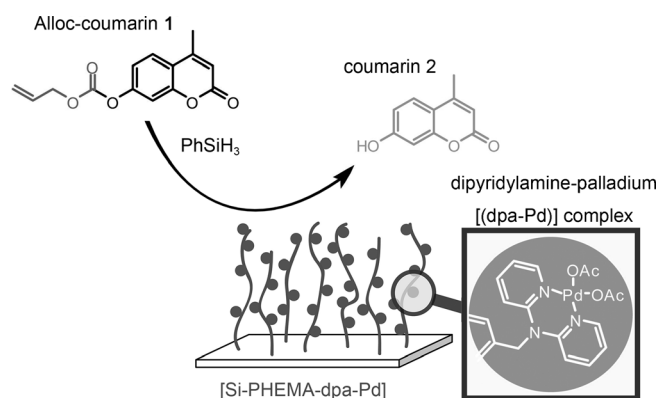
Planar surfaces hold unique, yet not well understood, potential in catalysis as a result of impressive performances observed upon decoration with monolayers of transition-metal complexes.<sup>[9]</sup> The possibility of assembling multifunctional

[a] Dr. A. E. Fernandes, Dr. A. Dirani, C. d'Haese, Dr. W. Guo, Dr. P. Hensenne, F. Nahra, Dr. X. Laloyaux, Prof. B. Nysten, Prof. O. Riant, Prof. A. M. Jonas  
Institute of Condensed Matter and Nanosciences  
Université catholique de Louvain  
Croix du Sud 1, 1348 Louvain-la-Neuve (Belgium)  
Fax: (+32)10-45-15-93  
E-mail: olivier.riant@uclouvain.be  
alain.jonas@uclouvain.be

[b] G. Deumer, Prof. V. Haufroid  
Louvain Centre for Toxicology and Applied Pharmacology  
Université catholique de Louvain  
Avenue Mounier 52, 1200 Woluwe-Saint-Lambert (Belgium)  
Fax: (+32)27-64-53-38

Supporting information for this article is available on the WWW under <http://dx.doi.org/10.1002/chem.201202531>.

catalytic surfaces<sup>[10]</sup> by means of lithographic techniques is a supplementary benefit of using planar supports. In our endeavor to explore the operation of catalytically active silicon surfaces, we envisioned the use of PBs as supports for homogeneous organometallic complexes. The systems presented herein were prepared by the complexation of  $[\text{Pd}(\text{OAc})_2]$  to pendant dipyrindylamine (dpa) ligands incorporated on to PBs of various thicknesses and evaluated in a model reaction based on the palladium(0)-mediated deprotection of Alloc-coumarin **1** (Scheme 1).<sup>[9e]</sup>



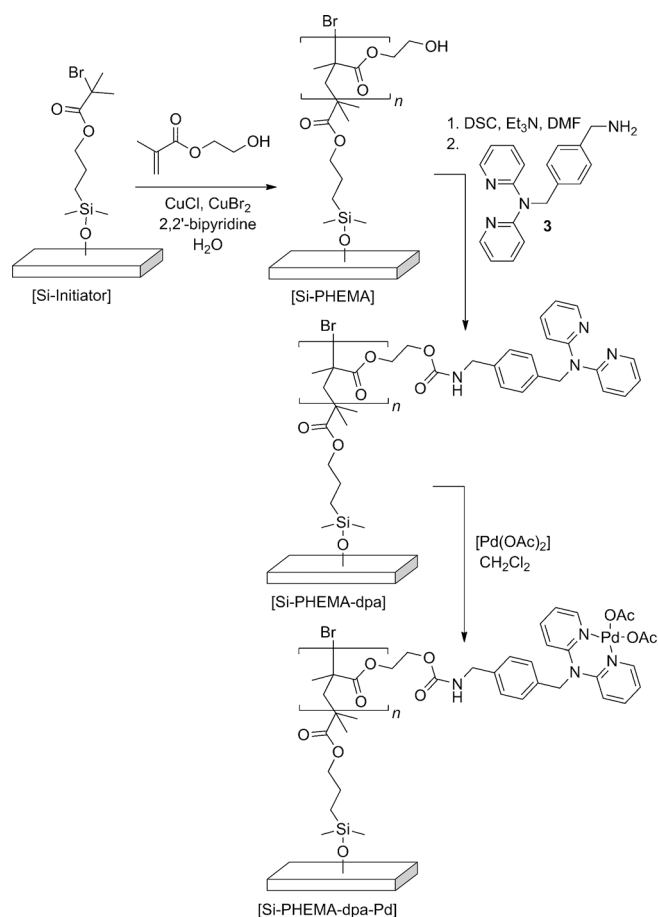
Scheme 1. Catalytic polymer brush on a planar silicon surface. A schematic of the palladium-catalyzed deprotection of Alloc-coumarin **1** is shown.

## Results and Discussion

In this report, poly(2-hydroxyethyl methacrylate) (PHEMA) PBs were grown on single-crystal silicon surfaces and post-decorated with 2,2'-dipyrindylamine (dpa) derivative **3** for the complexation of palladium catalysts (Scheme 2).<sup>[11]</sup>

PHEMA brushes were selected as they allow the simple introduction of suitable molecules by classical coupling with the hydroxy substituents of the lateral chains.<sup>[8a,12]</sup> An atom-transfer radical polymerization (ATRP) initiator silane was first self-assembled on to freshly cleaned silicon substrates by gas-phase silanization at 80 °C. The [Si-Initiator] samples were subsequently used for the surface-initiated atom-transfer radical polymerization (SI-ATRP)<sup>[8]</sup> of HEMA monomers. The pendant hydroxy groups of [Si-PHEMA] were then activated with *N,N'*-disuccinimidyl carbonate (DSC)<sup>[12]</sup> by using a standard protocol and the resulting samples directly reacted with dpa derivative **3** in DMF in the presence of  $\text{Et}_3\text{N}$  to afford [Si-PHEMA-dpa]. Finally, the substrates were immersed in a solution of  $[\text{Pd}(\text{OAc})_2]$  in  $\text{CH}_2\text{Cl}_2$  to give the catalytic surfaces [Si-PHEMA-dpa-Pd] after extensive washing in a Soxhlet apparatus.

The growth and modification of the PHEMA PBs were confirmed by ellipsometry, X-ray reflectivity (XRR), X-ray photoelectron spectroscopy (XPS), and inductively coupled plasma mass spectrometry (ICP-MS). A series of [Si-PHEMA] samples with dry thicknesses in the range of 10–80 nm were prepared by time-controlled SI-ATRP



Scheme 2. Stepwise synthesis of [Si-PHEMA-dpa-Pd] catalytic brushes.

(Figure 1). The samples were then postfunctionalized as described above to obtain [Si-PHEMA-dpa-Pd] surfaces. The evolution of the dry thickness of the layer gives a primary and rapid indication of the successful stepwise surface modification. The validity of the ellipsometric determination of the thickness was controlled by measuring the thicker brushes by XRR, which provides a model-independent thickness from interference fringes (see the Supporting Information).

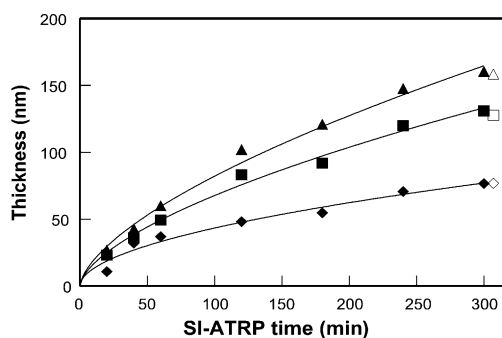


Figure 1. Evolution of the dry thickness of PBs following time-controlled SI-ATRP and subsequent postmodification. Diamonds: [Si-PHEMA]; squares: [Si-PHEMA-dpa]; triangles: [Si-PHEMA-dpa-Pd]. Closed symbols: ellipsometry; open symbols: XRR, displaced laterally by 7 min for clarity. The lines are fits to power laws ( $at^b$ ).

The increase in the thickness upon functionalization arises from the stretching of the individual chains to reduce steric congestion following the incorporation of the dpa ligand and palladium complexation. Accordingly, the thicknesses of the samples reported in this paper refer to the thickness of the parent [Si-PHEMA] brush, for example, 80[Si-PHEMA-dpa-Pd] refers to the postmodified 80 nm [Si-PHEMA] surface, but its actual thickness is around 150 nm. Based on the reported density of PHEMA and the molar volume of the repeat unit ( $102 \text{ cm}^3 \text{ mol}^{-1}$ ),<sup>[13]</sup> the thickness of the pristine brushes can be converted into the number of PHEMA repeat units per surface area (Figure 2).

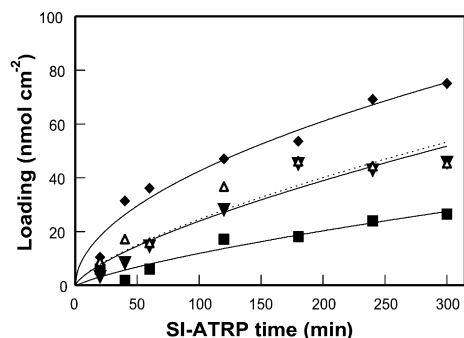


Figure 2. Evolution of the loadings following time-controlled SI-ATRP and subsequent postmodification.  $\blacklozenge$ : PHEMA repeat units;  $\blacksquare$ : grafted dpa **3**; and total palladium obtained from the thickness analysis ( $\blacktriangledown$ ) or from ICP-MS ( $\blacktriangle$ ). The lines are computed from the fits shown in Figure 1. The dotted line fits the palladium content determined from ICP-MS measurements.

XPS analysis of the thicker 80[Si-PHEMA] brush, which completely screens the substrate, provides an O/C ratio of 0.5, in good agreement with the brush composition. Incorporation of dpa ligand **3** results in the appearance of a nitrogen signal (ca. 400 eV) in the spectrum (Figure 3) with an experimental N/O ratio of 0.39 for the thicker 80[Si-PHEMA-dpa], which corresponds to 32% attachment of dpa **3** at the surface of the brush. The increment in the thickness following the grafting is 54 nm (Figure 1), which, upon division by the molar volume of the grafted unit ( $204.7 \text{ cm}^3 \text{ mol}^{-1}$ , estimated by the method of Fedors et al.),<sup>[14]</sup> provides  $26.5 \text{ nmol cm}^{-2}$  of dpa **3** (Figure 2), which indicates a 35% average grafting over the entire brush thickness, in good agreement with the XPS evaluation. The observed threshold of functionalization arises from the congestion caused by the covalent bonding of dpa **3**.<sup>[15]</sup> Thinner brushes, less than 40 nm, tend to have a lower grafting ratio of dpa **3**, probably due to the greater steric hindrance in the lower part of the brush. However, the accuracy of the measurements in these systems is also generally lower.

For the thicker brush, complexation with  $[\text{Pd}(\text{OAc})_2]$  afforded a Pd/N value of around 0.43, which is larger than the theoretical value (0.25) expected for the formation of a 1:1 complex between the pendant dpa ligand and  $[\text{Pd}(\text{OAc})_2]$ . This excess palladium presumably reflects the particularly

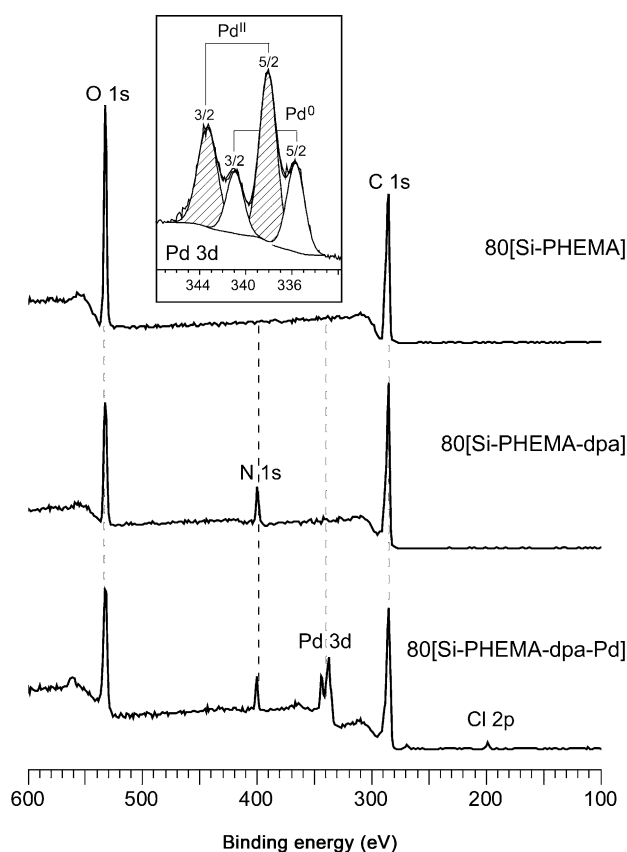


Figure 3. XPS spectra of 80[Si-PHEMA], 80[Si-PHEMA-dpa], and 80[Si-PHEMA-dpa-Pd]. The inset is an enlargement of the XPS palladium 3d region of the 80[Si-PHEMA-dpa-Pd] brush showing the ( $3d_{5/2}$ ;  $3d_{3/2}$ ) doublets of  $\text{Pd}^{\text{II}}$  and  $\text{Pd}^0$  in the sample.

coordinating nature of the PHEMA-dpa backbone, which bears a plethora of ester and carbamate donors in close proximity. A closer examination of the palladium 3d XPS region reveals the presence of two doublets ( $3d_{5/2}$ ;  $3d_{3/2}$ ) corresponding to  $\text{Pd}^{\text{II}}$  (343.3 and 338.1 eV) and  $\text{Pd}^0$  (340.9 and 335.7 eV) in a  $\text{Pd}^{\text{II}}/\text{Pd}^0$  ratio of around 1.9 (inset of Figure 3). Identical patterns were found for [Si-PHEMA-dpa-Pd] brushes of various thicknesses (see Table S2 and Figure S4 in the Supporting Information). Because the same observation was made in the starting  $[\text{Pd}(\text{OAc})_2]$  ( $\text{Pd}^{\text{II}}/\text{Pd}^0 = 1.8$ , see Table S2 and Figure S4) we ascribe the presence of  $\text{Pd}^0$  in the brush to the purity of the commercial  $[\text{Pd}(\text{OAc})_2]$ , as has recently been reported for other commercial palladium compounds.<sup>[16]</sup> Supplementary experiments ensured that XPS-induced reduction, although unlikely but observed in some rare cases,<sup>[17]</sup> did not occur at all in our analysis and thus may not be imputed to the presence of  $\text{Pd}^0$  in our samples. In addition, comparison of the experimental elementary ratios Pd/C=O (ca. 0.83) and  $\text{Pd}^{\text{II}}/\text{C}=\text{O}$  (ca. 0.53) in  $[\text{Pd}(\text{OAc})_2]$  (theoretical Pd/C=O=0.5) confirmed the coexistence of around  $2/3$   $[\text{Pd}(\text{OAc})_2]$  and  $1/3$   $\text{Pd}^0$  in the commercially available sample.

Taking these data into consideration, the refined  $\text{Pd}^{\text{II}}/\text{N}$  ratio is 0.28, which indicates a stoichiometric com-

plexation of the pendant dpa units of the brush. The presence of  $\text{Cl}^-$  in the XPS (ca. 200 eV) suggests a possible but limited exchange of acetate by chlorine anions ( $\text{Cl}^-/\text{Pd}^{\text{II}} = 0.48$ ) for around 25 % of the  $\text{Pd}^{\text{II}}$  atoms.

Detailed analysis of the N1s XPS region before and after the incorporation of palladium also provided evidence for the complexation of the dpa motifs. A shift of the pyridine nitrogen atoms of [Si-PHEMA-dpa] (ca. 398.9 eV) towards higher binding energies (ca. 400.1 eV), and thus towards an electron-poor state, is consistent with coordination to palladium (see Table S3 and Figure S5 in the Supporting Information).<sup>[18]</sup>

Based on the molar volumes of  $[\text{Pd}(\text{OAc})_2]$  ( $102.5 \text{ cm}^3 \text{ mol}^{-1}$ ),  $\text{PdCl}_2$  ( $44.3 \text{ cm}^3 \text{ mol}^{-1}$ ), and  $\text{Pd}^0$  ( $8.9 \text{ cm}^3 \text{ mol}^{-1}$ ) and on the XPS-determined composition for  $[\text{Pd}(\text{OAc})_2]/\text{PdCl}_2/\text{Pd}^0$  of 0.75:0.25:0.53, which corresponds to an average volume of  $60.7 \text{ cm}^3 \text{ mol}^{-1}$  of added palladium, the difference of thickness of 28 nm resulting from palladium addition can be converted into  $46 \text{ nmol cm}^{-2}$  of palladium in the brush, which compares well with the value of  $45 \text{ nmol cm}^{-2}$  obtained by ICP-MS. Similar good agreement was found for other brush thicknesses (Figure 2), which adds support to our analysis.

Because ICP-MS provides a direct quantitative analysis of the total palladium content in the brushes, it will be used in the following. Analysis of the [Si-PHEMA-dpa-Pd] series shown in Figure 1 (ca. 20–160 nm) reveals a near-linear correlation between thickness and palladium content (Figure 4), which indicates that the dpa and palladium moieties diffuse and graft similarly in thin and thick brushes.

This correlation demonstrates the robustness of the post-modification sequence presented herein and the possibility of relatively precisely adjusting the catalytic performances of PB-supported catalysts.<sup>[7d,g,h]</sup> It also confirms the coordinating nature of the PHEMA-dpa core as being responsible for excessive palladium incorporation in comparison with the amount of dpa ligand in the brush.

To study the effect of PB thickness and palladium loading on catalytic activity, a series of [Si-PHEMA] samples with thicknesses of around 30, 40, and 80 nm were prepared, with a good thickness distribution within the series (see Figure S1 in the Supporting Information), and functionalized. The pal-

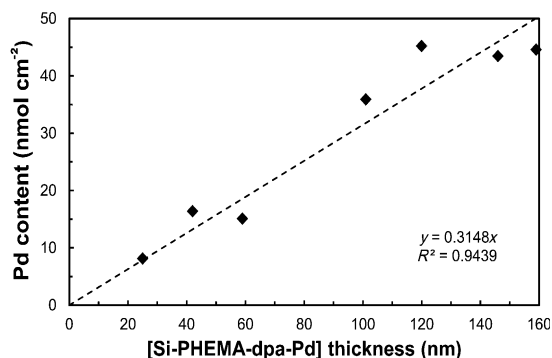


Figure 4. Correlation between [Si-PHEMA-dpa-Pd] thickness and palladium content (as determined by ICP-MS).

ladium content of the corresponding PBs was approximated by extrapolation of the ICP-MS calibration curve shown in Figure 2 (ca. 12.1, 18.6, and  $46.9 \text{ nmol cm}^{-2}$  respectively). The activities of the different surfaces were examined in the fluorogenic deprotection of  $1 \times 10^{-5} \text{ mol}$  of Alloc-coumarin **1** (Scheme 1, Table 1). Furthermore, to access additional, higher, substrate-to-catalyst ratios (S/C) in a straightforward manner, surfaces with areas of 1, 0.5, and  $0.25 \text{ cm}^2$  were tested for each thickness.

Table 1. Catalytic activity of [Si-PHEMA-dpa-Pd] in the deprotection of  $1 \times 10^{-5} \text{ mol}$  Alloc-coumarin **1**.

Sample	Surface area [ $\text{cm}^2$ ]	S/C <sup>[a]</sup>	Conversion [%] <sup>[b]</sup>	TON <sup>[c]</sup>
1 80[Si-PHEMA-dpa-Pd]	1	213	94	200
2	0.5	426	96	409
3	0.25	852	95	809
4 40[Si-PHEMA-dpa-Pd]	1	538	96	516
5	0.5	1076	96	1033
6	0.25	2152	96	2066
7 30[Si-PHEMA-dpa-Pd]	1	826	96	793
8	0.5	1652	98	1619
9	0.25	3304	96	3172

[a] Substrate-to-catalyst ratio. [b] Conversion after 20 h, as determined by  $^1\text{H}$  NMR spectroscopy. [c] Turnover number.

All the samples showed remarkable performances with the quantitative formation of free coumarin **2**. A maximal turnover number (TON) of around 3172 was recorded with the  $0.25 \text{ cm}^2$  30[Si-PHEMA-dpa-Pd] sample (Table 1, entry 9).

To assess the full potential of the catalytic brushes, the catalyzed reactions were also conducted with  $1 \times 10^{-4} \text{ mol}$  of Alloc-coumarin **1** (Table 2). A progressive decrease in activity was recorded and directly related to the diminution of the surface area and PB thickness, and thus to the palladium content engaged in the reactions. Interestingly, the  $0.25 \text{ cm}^2$  40[Si-PHEMA-dpa-Pd] brushes afforded the highest TON of around 4086 (entry 7) whereas the  $1 \text{ cm}^2$  80[Si-PHEMA-dpa-Pd] surface gave the best conversion of around 51 % (entry 1). In addition, the samples prepared by the direct incorporation of palladium into nonfunctionalized PHEMA brushes ([Si-PHEMA-Pd], Table 2, entries 4, 8, and 12) showed limited reactivity compared with their [Si-PHEMA-dpa-Pd] counterparts, with no particular influence of PB thickness. Palladium may thus be poorly adsorbed on to the pristine PHEMA brushes and only complexes (and entraps) dpa-modified PBs, as previously noted.

Figure 5 allows a comprehensive visualization of the catalytic properties of our PBs. Quantitative conversions can be attained below a threshold S/C ratio of around 3500, above which conversions decrease as S/C increases. Similarly, the evolution of TONs against S/C ratios confirmed an asymptotic limit TON of around 3500.

Intuitively and experimentally, the thickest surfaces, that is, those having the highest palladium contents, prove to be the most active in terms of conversion. However, the TONs

Table 2. Catalytic activity of [Si-PHEMA-dpa-Pd] in the deprotection of  $1 \times 10^{-4}$  mol Alloc-coumarin **1**.

Sample	Surface area [cm <sup>2</sup> ]	S/C <sup>[a]</sup>	Conversion [%] <sup>[b]</sup>	TON <sup>[c]</sup>	
1	80[Si-PHEMA-dpa-Pd]	1	2132	51	1087
2		0.5	4264	39	1663
3		0.25	8528	29	2473
4	80[Si-PHEMA-Pd]	1	n.d. <sup>[d]</sup>	7	n.d. <sup>[d]</sup>
5	40[Si-PHEMA-dpa-Pd]	1	5376	40	2150
6		0.5	10752	25	2688
7		0.25	21504	19	4086
8	40[Si-PHEMA-Pd]	1	n.d. <sup>[d]</sup>	9	n.d. <sup>[d]</sup>
9	30[Si-PHEMA-dpa-Pd]	1	8264	25	2066
10		0.5	16528	15	2479
11		0.25	33056	8	2644
12	30[Si-PHEMA-Pd]	1	n.d. <sup>[d]</sup>	4	n.d. <sup>[d]</sup>

[a] Substrate-to-catalyst ratio. [b] Conversion after 20 h, as determined by <sup>1</sup>H NMR spectroscopy. [c] Turnover number. [d] Not determined.

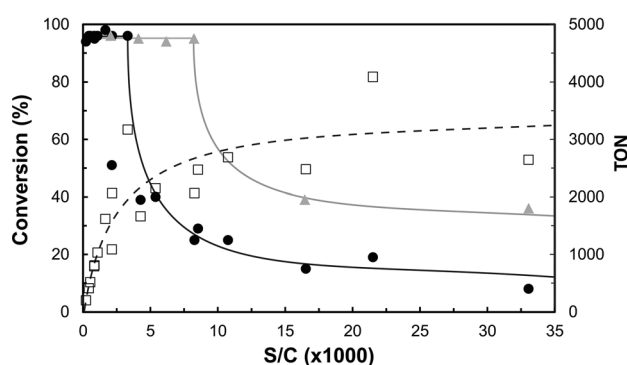


Figure 5. Conversion (●) and TON (□) versus S/C ratios for [Si-PHEMA-dpa-Pd] surfaces. ▲ represent conversions obtained by using the homogeneous [Pd(OAc)<sub>2</sub>] catalyst under similar conditions. Black line: evolution of the conversion for [Si-PHEMA-dpa-Pd]; grey line: evolution of conversion for homogeneous [Pd(OAc)<sub>2</sub>]; black dashed line: evolution of TON for [Si-PHEMA-dpa-Pd].

are more difficult to apprehend. For  $S/C < 3500$ , the TONs naturally follow the increase in the  $S/C$  ratios directly linked to the modification of the surface area and PB thickness.

For example, increasing the  $S/C$  ratio by a factor of two results in a proportional augmentation in the TONs (Table 1). When pushing the system above its limits ( $S/C > 3500$ , Table 2), although a TON of around 3500 should theoretically be measured in every case, a discrepancy is observed and, for an identical surface area, higher TONs are recorded for the thinnest PBs. These observations suggest that only a portion of the thickest catalytic brushes seems available for the reaction to take place. Facilitated diffusion of reactants and products in the thinnest PBs also has to be considered.

The influence of the solvent was not examined in this work as we have previously observed<sup>[9]</sup> that the outcome of our model reaction is strongly dependent on the nature of the solvent. Thus, this renders the approximation of solvent-triggered ar-

chitectural effects (swollen/collapsed PBs) particularly complicated.

Finally, the recyclability of our supported catalysts was explored by physically transferring the surface (after copious rinsing with  $\text{CH}_2\text{Cl}_2$ ) to a new reaction (Table 3). For iterative runs, the activities of the catalytic PBs progressively drop. This tendency is even more pronounced when working at larger  $S/C$  ratios, that is, for the smallest and thinnest [Si-PHEMA-dpa-Pd] surfaces. Total TONs are finally  $\lesssim 3500$ , consistent with the observed limit of our catalyst. As previously observed,<sup>[9]</sup> the progressive deactivation of the catalytic PBs is mainly attributed to the gradual leaching of palladium. A simple regeneration process allowed used samples, after being reloaded by immersion in [Pd(OAc)<sub>2</sub>] solution, to almost recover their initial potential. XPS analysis of used samples confirmed palladium leaching as being the main cause of catalyst deactivation.

Homogeneous experiments with commercially available [Pd(OAc)<sub>2</sub>] revealed quantitative transformations when using palladium contents greater than around 0.01 mol% (0.03 mol% for [Si-PHEMA-dpa-Pd]) and a maximum TON of around 12000 (given the XPS-determined composition of [Pd(OAc)<sub>2</sub>]; Figure 5). Thus immobilization of palladium catalysts on to polymer brushes appears at first sight detrimental to their activity owing presumably to accessibility and diffusion issues.

The poor reusability of our surfaces prompted us to elucidate the exact nature of the catalytic species involved, that is, whether the brushes work as purely heterogeneous catalysts or as catalytic reservoirs.<sup>[7b]</sup> With this aim, [Si-PHEMA-dpa-Pd] samples were first treated with  $\text{PhSiH}_3$  in  $\text{CH}_2\text{Cl}_2/\text{EtOH}$  to generate the Pd<sup>0</sup> species. After 20 h, the surfaces were removed and engaged in the catalytic deprotection of Alloc-coumarin **1** ( $1 \times 10^{-4}$  mol, 10 equiv  $\text{PhSiH}_3$ ). In addition, the activities of the remaining solutions were tested similarly (Table 4).

Table 3. Recyclability of [Si-PHEMA-dpa-Pd] catalytic brushes.

Amount of <b>1</b> [mol]	Sample	Surface area [cm <sup>2</sup> ]	S/C <sup>[a]</sup>	Conversion [%] <sup>[b]</sup> for run					Total TON <sup>[c]</sup>
				1	2	3	4	5	
1	$1 \times 10^{-5}$	80[Si-PHEMA-dpa-Pd]	213	94	96	30	15	11	524
2			0.5	426	96	97	32	8	993
3			0.25	852	95	74	12	7	1602
4		40[Si-PHEMA-dpa-Pd]	1	538	96	24	29	17	995
5			0.5	1076	96	15	11	–	1313
6			0.25	2152	96	19	9	–	2668
7		30[Si-PHEMA-dpa-Pd]	1	826	96	17	12	–	1033
8			0.5	1652	98	15	12	–	2065
9			0.25	3304	96	10	–	–	3502
10	$1 \times 10^{-4}$	80[Si-PHEMA-dpa-Pd]	1	2132	51	10	–	–	1298
11			0.5	4264	39	7	–	–	1958
12			0.25	8528	29	8	–	–	3149

[a] Substrate-to-catalyst ratio. [b] Conversion after 20 h, as determined by <sup>1</sup>H NMR spectroscopy. [c] Total turnover number.

Table 4. Unraveling the catalytic nature of [Si-PHEMA-dpa-Pd].<sup>[a]</sup>

Sample	S/C <sup>[b]</sup>	Conversion [%] <sup>[c]</sup>	Conversion [%] <sup>[d]</sup>	Conversion [%] <sup>[e]</sup>
80[Si-PHEMA-dpa-Pd]	2132	51 (96)	12	95
40[Si-PHEMA-dpa-Pd]	5376	40 (95)	7	91
30[Si-PHEMA-dpa-Pd]	8264	25 (95)	7	21

[a] 1 cm<sup>2</sup> [Si-PHEMA-dpa-Pd], 1 × 10<sup>-4</sup> mol Alloc-coumarin **1**, 20 h. [b] Substrate-to-catalyst ratio. [c] No initial treatment. Conversions in parentheses correspond to homogeneous controls with [Pd(OAc)<sub>2</sub>]. [d] Surfaces treated with PhSiH<sub>3</sub> prior to catalysis. [e] Activity of the remaining solution resulting from the treatment of [Si-PHEMA-dpa-Pd] with PhSiH<sub>3</sub>.

Accordingly, surfaces treated (PhSiH<sub>3</sub>) as stated above showed no or poor activity (7–12%), which suggests that all the catalytic species had leached into the reducing solution. Indeed, the solutions resulting from the initial treatment of the [Si-PHEMA-dpa-Pd] samples were found to be highly active, with conversions almost similar to those of homogeneous controls with [Pd(OAc)<sub>2</sub>]. The difference between treated/untreated [Si-PHEMA-dpa-Pd] and homogeneous controls suggests that the reaction most probably occurs within or in the vicinity of the brushes, which thus restrains the activity to a level comparable to the homogeneous [Pd(OAc)<sub>2</sub>] counterparts.

Therefore these experiments together with the recyclability tests (Table 3) and XPS studies have revealed that the catalytic brushes presented herein function as forms of catalytic reservoirs releasing active palladium species into solution as a result of the poor stability of [dpa-Pd<sup>0</sup>] complexes compared with [dpa-Pd<sup>II</sup>].

## Conclusion

PHEMA polymer brushes have been used for the immobilization of dpa-palladium complexes on to flat silicon oxide to prepare catalytically active surfaces.

We have demonstrated that the palladium concentration can be well adjusted by using PBs of various thicknesses attainable by time-controlled SI-ATRP. Our system relies on the simple and robust postfunctionalization of the pendant hydroxy groups of the PHEMA PBs by conventional activation and coupling chemistry.

A systematic study of our catalytic brushes (thickness, S/C screenings, recyclability, leaching test) has unambiguously revealed that our system functions as a reservoir that progressively releases catalytically active species into solution. The PB reservoir shows a limiting TON of around 3500, less than the homogeneous controls with [Pd(OAc)<sub>2</sub>], which indicates that the reaction occurs in the vicinity of the brush framework and thus analogous activity is hindered. The thickest surfaces offered the highest conversions due to increased palladium content in the brushes. When working under “extreme” conditions (S/C > 3500), the thinnest surfaces proved to be the most effective in terms of TON as a result of catalyst release by enhanced diffusion out of the brushes.

The preliminary study reported herein represents, to the best of our knowledge, the first example of a transition-metal catalyst immobilized on PBs prepared from single-crystal silicon surfaces. Although our catalytic system needs further improvement, the PBs represent an appealing platform for the construction of innovative catalytic devices. The possibility of reversibly collapsing/stretching PBs in response to external stimuli<sup>[19]</sup> has tremendous potential for the assembly of switchable catalytic surfaces<sup>[20]</sup> to achieve precise control over chemical processes.<sup>[21]</sup>

Further studies will be dedicated to configuring adaptive, robust, heterogeneous catalytic systems from planar silicon surfaces. The deactivation can be attributed to the strong reducing media (PhSiH<sub>3</sub>, used as a nucleophile and reducing agent) that keep the palladium species in a low oxidation state. Decoordination from the weak low-oxidation-state coordinating ligand dpa is then favored and leads most probably to the formation of palladium particles. Model reactions that do not involve the formation of Pd<sup>0</sup> species (such as Michael addition or nitro-aldol reaction) should give more robust catalytic systems and will be investigated in the near future.

## Experimental Section

**General:** Reagents were obtained from commercial sources and used without further purification. All reactions were carried out under N<sub>2</sub> or argon. ROCC 60 granular silica gel (40–63 μm, 230–400 mesh ASTM) was employed for column chromatography. Single-side-polished silicon wafers were purchased from ACM (France) with (100) orientation. Milli-Q water (resistivity 18.2 MΩ cm) was obtained from the Millipore system (Elga Purelab Ultra). All reaction vessels were cleaned prior to use by immersion in a hot, freshly prepared piranha solution (H<sub>2</sub>SO<sub>4</sub> (98%)/H<sub>2</sub>O<sub>2</sub> (30%)) and then extensively washed with Milli-Q water and dried in an oven. (**Caution!** Piranha solution is an extremely strong oxidant and should be handled only with the proper equipment.)

Ellipsometry (Uvisel, Horiba-Jobin-Yvon, France) was performed at an incidence angle of 70° and in a wavelength range of 400–850 nm. The ellipsometric data were fitted by using the DeltaPsi 2 software accompanying the measuring apparatus. The ellipsometric model consists of three layers: Silicon (bulk), native silicon oxide (1.5 nm thickness), and a polymer brush. The complex indices of refraction of silicon and native SiO<sub>2</sub> were taken from tabulated data provided by the manufacturer. The complex indices of refraction of the brushes,  $n-jk$ , was modeled by a transparent Cauchy layer with  $n(\lambda) = A + B\lambda^{-2} + C\lambda^{-4}$  and  $k(\lambda) = 0$ , with  $A$ ,  $B$ , and  $C$  three fitted parameters. X-ray reflectivity (XRR) measurements were carried out with a modified Siemens D5000 2-circle goniometer (0.002° positioning accuracy). X-rays of wavelength 0.15418 nm (Cu<sub>Kα1</sub>) were obtained from a Rigaku rotating anode operated at 40 kV and 300 mA, fitted with a collimating mirror (Osmic, Japan) delivering a close-to-parallel beam with around 0.0085° vertical angular divergence. X-ray photoelectron spectroscopy (XPS) measurements were performed on a SSX 100/206 photoelectron spectrometer from Surface Science Instruments (USA) equipped with a monochromatized microfocused aluminium X-ray source ( $h\nu = 1486.6$  eV) operated at 20 mA and 10 kV. All binding energies are referenced to the C–(C,H) component of the carbon 1s peak fixed at 284.8 eV. The base pressure in the spectrometer was in the low 10<sup>-8</sup> Torr range. Quantitative information was obtained from the photoemission peak areas of each element normalized according to acquisition parameters and sensitivity factors provided by the manufacturer. Peak decomposition was achieved with the Casa XPS software (Casa Software Ltd., UK). Inductively coupled plasma mass spectroscopy (ICP-

MS) was performed on an Agilent Quadrupole inductively coupled plasma mass spectrometer. The samples were treated with ultrapure aqua regia (3:1 concentrated HCl/HNO<sub>3</sub>) and the resulting solution was diluted 10 times prior to analysis. (**Caution!** Aqua regia is a very corrosive oxidizing agent, which should be handled with great care.) NMR spectra were recorded on a Bruker-300 spectrometer. Mass spectra were obtained by using a ThermoFinnigan LCQ Quantum spectrometer.

**Silanization:** The silicon wafers were cleaned by plasma etching and then immediately installed in a Teflon holder and transferred into a Schlenk tube. The whole system was sealed and heated at 80 °C. Three cycles of vacuum/N<sub>2</sub> were performed. The ATRP initiator silane (15 μL) was then injected and the reaction was carried out at 80 °C for 2 h. The silanized silicon wafers were removed, rinsed with toluene, and dried under a flow of nitrogen.

**Growth of poly(2-hydroxyethyl methacrylate) (PHEMA) polymer brushes by surface-initiated atom-transfer radical polymerization (SI-ATRP):** HEMA (8 mL) monomer was dissolved in deionized water (8 mL) and CuCl (110 mg), CuBr<sub>2</sub> (72 mg), and bipyridine (488 mg) were added. The vessel was then sealed and N<sub>2</sub> was bubbled. The solution was stirred under N<sub>2</sub> for 45 min until a homogeneous dark-brown solution formed. A series of Schlenk tubes containing one [Si-Initiator] sample each were sealed and subjected three vacuum/N<sub>2</sub> cycles. The growth of the polymer brushes was initiated by the injection of the previously described solution (2.5 mL solution per sample). The reactions were performed for determined periods of time to give PBs of various thicknesses. The [Si-PHEMA] surfaces were recovered, rinsed twice with methanol and deionized water, and dried under a flow of nitrogen.

**Incorporation of the dpa ligand 3:** Reactions were performed in a glove box. [Si-PHEMA] was first activated prior to coupling with **3**. The [Si-PHEMA] surfaces were immersed in a solution of *N,N'*-disuccinimidyl carbonate (DSC; 0.10 mmol per sample) and Et<sub>3</sub>N (0.20 mmol per sample) in DMF (2 mL per sample) for 24 h. The samples were then removed, washed with DMF, and immersed into a solution containing dpa ligand **3** (0.03 mmol per sample) and Et<sub>3</sub>N (0.10 mmol per sample) in DMF (1.5 mL per sample). After 24 h of reaction, the samples were removed and thoroughly washed with CH<sub>2</sub>Cl<sub>2</sub> to give [Si-PHEMA-dpa] surfaces.

**Incorporation of [Pd(OAc)<sub>2</sub>]:** Reactions were performed in a glove box. Prior to complexation, the backsides of the samples were covered with a layer of poly(vinylidene difluoride) (PVdF). The [Si-PHEMA-dpa] surfaces were immersed in a solution of [Pd(OAc)<sub>2</sub>] (0.05 mmol per sample) in CH<sub>2</sub>Cl<sub>2</sub> (3 mL per sample) for 2 h. The samples were then removed and washed with CH<sub>2</sub>Cl<sub>2</sub> in a Soxhlet apparatus overnight to obtain the [Si-PHEMA-dpa-Pd] catalysts.

**Catalysis:** The reactions were performed in freshly cleaned (piranha) Schlenk tubes. Appropriate stock solutions of Alloc-coumarin **1** were prepared prior to catalysis (CH<sub>2</sub>Cl<sub>2</sub>/EtOH, 1:1, v/v). A [Si-PHEMA-dpa-Pd] surface was immersed in coumarin **1** (1 mL) and PhSiH<sub>3</sub> (10 equiv) was added. The system was kept under argon for 20 h without stirring. Conversions were determined by <sup>1</sup>H NMR spectroscopy.<sup>[9a]</sup>

## Acknowledgements

The authors gratefully acknowledge access to the SUCH and ASM platforms of IMCN. BN is a Senior Research Associate of the FRS-FNRS. Financial support was provided by the Communauté Française de Belgique (ARC 06-11/339), the Belgian Federal Science Policy (IAP-PAI P6/27), and the FRS-FNRS. Michel Genet is gratefully acknowledged for discussions on the XPS data.

[1] S. T. Milner, *Science* **1991**, *251*, 905–914.

[2] a) S. Morsch, W. C. Schofield, J. P. Badyal, *Langmuir* **2010**, *26*, 12342–12350; b) Y. Roiter, I. Minko, D. Nykypanchuk, I. Tokarev, S. Minko, *Nanoscale* **2012**, *4*, 284–292.

- [3] L. Li, W. Hu, L. Chi, H. Fuchs, *J. Phys. Chem. B* **2010**, *114*, 5315–5319.
- [4] W. Senaratne, L. Andruzzi, C. K. Ober, *Biomacromolecules* **2005**, *6*, 2427–2448.
- [5] a) S. Tugulu, A. Arnold, I. Sielaff, K. Johnsson, H.-A. Klok, *Biomacromolecules* **2005**, *6*, 1602–1607; b) K. Glinel, A. M. Jonas, T. Jouenne, J. Leprince, L. Galas, W. T. S. Huck, *Bioconjugate Chem.* **2009**, *20*, 71–77; c) X. Laloyaux, E. Fautré, T. Blin, V. Purohit, J. Leprince, T. Jouenne, A. M. Jonas, K. Glinel, *Adv. Mater.* **2010**, *22*, 5024–5028.
- [6] S. Samanta, J. Locklin, *Langmuir* **2008**, *24*, 9558–9565.
- [7] a) J. Huang, X. Li, Y. Zheng, Y. Zhang, R. Zhao, X. Gao, H. Yan, *Macromol. Biosci.* **2008**, *8*, 508–515; b) B. Zhao, X. Jiang, D. Li, X. Jiang, T. O'Lenick, B. Li, C. Y. Li, *J. Polym. Sci. Part A* **2008**, *46*, 3438–3446; c) C. S. Gill, K. Venkatasubbaiah, N. T. S. Phan, M. Weck, C. W. Jones, *Chem. Eur. J.* **2008**, *14*, 7306–7313; d) F. Costantini, W. P. Bula, R. Salvio, J. Huskens, H. J. G. E. Gardeniens, D. N. Reinhoudt, W. Verboom, *J. Am. Chem. Soc.* **2009**, *131*, 1650–1651; e) C. S. Gill, W. Long, C. W. Jones, *Catal. Lett.* **2009**, *131*, 425–431; f) A. Schätz, T. R. Long, R. N. Grass, W. J. Stark, P. R. Hanson, O. Reiser, *Adv. Funct. Mater.* **2010**, *20*, 4323–4328; g) F. Costantini, E. M. Benetti, D. N. Reinhoudt, J. Huskens, G. J. Vancso, W. Verboom, *Lab Chip* **2010**, *10*, 3407–3412; h) F. Costantini, E. M. Benetti, R. M. Tiggelaar, H. J. G. E. Gardeniens, D. N. Reinhoudt, J. Huskens, G. J. Vancso, W. Verboom, *Chem. Eur. J.* **2010**, *16*, 12406–12411; i) M. Zeltner, A. Schätz, M. L. Hefti, W. J. Stark, *J. Mater. Chem.* **2011**, *21*, 2991–2996; j) W. Long, C. W. Jones, *ACS Catal.* **2011**, *1*, 674–681.
- [8] a) R. Barbey, L. Lavanant, D. Paripovic, N. Schüwer, C. Sugnaux, S. Tugulu, H.-A. Klok, *Chem. Rev.* **2009**, *109*, 5437–5527; b) S. V. Orski, K. H. Fries, S. K. Sontag, J. Locklin, *J. Mater. Chem.* **2011**, *21*, 14135–14149.
- [9] a) M. G. L. Petrucci, A. K. Kakkar, *J. Chem. Soc., Chem. Commun.* **1995**, 1577–1578; b) M. G. L. Petrucci, A. K. Kakkar, *Chem. Mater.* **1999**, *11*, 269–276; c) A. K. Kakkar, *Chem. Rev.* **2002**, *102*, 3579–3588; d) B. A. Harper, D. A. Knight, C. George, S. L. Brandow, W. J. Dressick, C. S. Dalcey, T. L. Schull, *Inorg. Chem.* **2003**, *42*, 516–524; e) K. Hara, S. Tayama, H. Kano, T. Masuda, S. Takakusagi, T. Kondo, K. Uosaki, M. Sawamura, *Chem. Commun.* **2007**, 4280–4282; f) K. Hara, R. Akiyama, S. Takakusagi, K. Uosaki, T. Yoshino, H. Kagi, M. Sawamura, *Angew. Chem.* **2008**, *120*, 5709–5712; *Angew. Chem. Int. Ed.* **2008**, *47*, 5627–5630; g) A. Fernandes, P. Hensenne, B. Mathy, W. Guo, B. Nysten, A. M. Jonas, O. Riant, *Chem. Eur. J.* **2012**, *18*, 788–792.
- [10] D. Kisailus, Q. Truong, Y. Amemiya, J. C. Weaver, D. E. Morse, *Proc. Natl. Acad. Sci. USA* **2006**, *103*, 5652–5657.
- [11] a) M. R. Buchmeiser, S. Lubbad, M. Mayr, K. Wurst, *Inorg. Chim. Acta* **2003**, *345*, 145–153; b) S. Fakhri, W. C. Tung, D. Eierhoff, C. Mock, B. Krebs, *Z. Anorg. Allg. Chem.* **2005**, *631*, 1397–1402; c) B. Antonoli, D. J. Bray, J. K. Clegg, K. Gloe, K. Gloe, A. Jäger, K. A. Jolliffe, O. Kataeva, L. F. Lindoy, P. J. Steel, C. J. Sumby, M. Wenzel, *Polyhedron* **2008**, *27*, 2889–2898.
- [12] a) B. S. Lee, Y. S. Chi, K.-B. Lee, Y.-G. Kim, I. S. Choi, *Biomacromolecules* **2007**, *8*, 3922–3929; b) S. Diamanti, S. Arifuzzaman, A. Elsen, J. Genzer, R. A. Vaia, *Polymer* **2008**, *49*, 3770–3779; c) S. M. Lane, Z. Kuang, J. Yom, S. Arifuzzaman, J. Genzer, B. Farmer, R. Naik, R. A. Vaia, *Biomacromolecules* **2011**, *12*, 1822–1830.
- [13] N. A. Peppas, H. J. Moynihan, L. M. Lucht, *J. Biomed. Mater. Res.* **1985**, *19*, 397–411.
- [14] R. F. Fedors, *Polym. Eng. Sci.* **1974**, *14*, 147–154.
- [15] V. A. Baulin, E. B. Zhulina, A. Halperin, *J. Chem. Phys.* **2003**, *119*, 10977–10989.
- [16] S. S. Zaleskiy, V. P. Ananikov, *Organometallics* **2012**, *31*, 2302–2309.
- [17] a) J. El Fallah, L. Hilaire, M. Roméo, F. Le Normand, *J. Electron Spectrosc. Relat. Phenom.* **1995**, *73*, 89–103; b) C. C. Chusuei, M. A. Brokkshier, D. W. Goodman, *Langmuir* **1999**, *15*, 2806–2808.
- [18] a) J. P. Mathew, M. Srinivasan, *Eur. Polym. J.* **1995**, *31*, 835–839; b) A. K. Zharmagambetova, V. A. Golodov, Y. P. Saltykov, *J. Mol. Catal.* **1989**, *55*, 406–414; c) G. B. Onoa, V. Moreno, M. Font-

- Bardia, X. Solans, J. M. Pérez, C. Alonso, *J. Inorg. Biochem.* **1999**, *75*, 205–212.
- [19] a) X. Laloyaux, B. Mathy, B. Nysten, A. M. Jonas, *Macromolecules* **2010**, *43*, 7744–7751; b) X. Laloyaux, B. Mathy, B. Nysten, A. M. Jonas, *Langmuir* **2010**, *26*, 838–847.
- [20] R. S. Stoll, S. Hecht, *Org. Lett.* **2009**, *11*, 4790–4793.
- [21] a) H. J. Yoon, J. Kuwabara, J.-H. Kim, C. A. Mirkin, *Science* **2010**, *330*, 66–69; b) Y. Sohtome, S. Tanaka, K. Takada, T. Yamaguchi, K. Nagasawa, *Angew. Chem.* **2010**, *122*, 9440–9443; *Angew. Chem. Int. Ed.* **2010**, *49*, 9254–9257; c) J. Wang, B. L. Feringa, *Science* **2011**, *331*, 1429–1432; d) V. Blanco, A. Carlone, K. D. Hänni, D. A. Leigh, B. Lewandowski, *Angew. Chem.* **2012**, *124*, 5256–5259; *Angew. Chem. Int. Ed.* **2012**, *51*, 5166–5169; e) D. Wilson, N. R. Branda, *Angew. Chem.* **2012**, *124*, 5527–5530; *Angew. Chem. Int. Ed.* **2012**, *51*, 5431–5434.

Received: July 16, 2012  
Published online: October 2, 2012